speedam
Capri, Italy
5-7 June 1996

Symposium on
Power Electronics, Industrial Drives, Power Quality, Traction Systems

STUDY OF A PERMANENT-MAGNET EXCITED AXIAL-FLUX ELECTROMAGNETIC DIFFERENTIAL MOTOR FOR WHEEL DIRECT DRIVE APPLICATION

F. Caricchi (*), F. Crescimbini (*), T.A. Lipo (**)

(*) *University of Rome "La Sapienza"*
Dept. of Electrical Engineering
Via Eudossiana, 18
00184 Rome, ITALY

(**) *University of Wisconsin - Madison*
Dept. of Electrical & Computer Engineering
1415 Johnson Drive, Madison,
WI 53706-1691, USA

Abstract

This paper describes a newly-conceived topology of axial-flux motor which has a single slotless toroidal stator, two PM rotor discs and two cage-winding rotor discs. The cage-winding rotors are mounted on individual, independent shafts directly driving two wheels of an electric vehicle. The paper discusses the basic operating principle of such an original machine, and equivalent circuits for the study of steady-state and transient operation are derived. Finally, results of a computer simulation are used to discuss the machine behaviour when operated as wheel direct drive motor.

1. INTRODUCTION

In electric vehicle applications, the mechanical transmission system used in thermal-engine vehicles can be avoided by using electric motors designed for the direct driving of the vehicle wheels. For such a low-speed high-torque application, axial-flux PM motor drives have been recently proposed [1,2] because of desirable characteristics such as high torque-to-weight ratio and efficiency.

This paper describes an original axial-flux motor which has a single slotless toroidal stator, two PM rotor discs and two cage-winding rotor discs. As shown in Fig. 1, the stator is sandwiched between the two PM rotors, and all this as a whole is sandwiched between the two cage-winding rotors which are mounted on individual, independent shafts to directly drive two wheels of an electrical vehicle. Thereby, the proposed axial-flux machine combines in a single motor drive the function

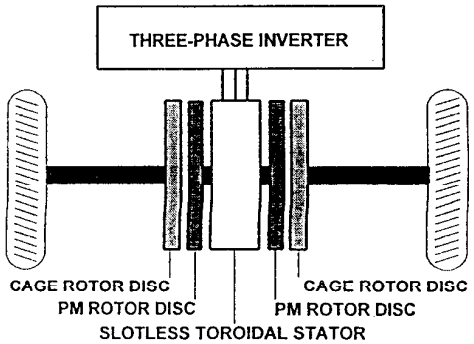

Fig. 1 Wheel Direct Drive with Axial Flux PM Excited Electromagnetic Differential Motor.

of both the engine and the differential of a conventional vehicle, and in comparison with wheel direct drives which require as much power converters as the driving wheels, one significant advantage of the drive arrangement shown in Fig. 1 is that only a single power converter is needed for the supply of the machine.

Early studies of ac electric motors having a single stator and two rotors were developed by considering the conventional arrangement of cylindrical induction and synchronous type rotors with radial airgap flux [3]. More recently, design and performance of a disc-type induction machine having two cage-winding rotors and single stator with two separate windings connected in series were discussed in [4], and a machine structure same as in [4] but with a stator having a single winding for shorter length of the end-windings was proposed in [5].

The machine topology presented in this paper has some similarities with the machines proposed in [3, 4, 5], but it uses permanent magnet excitation in an axial configuration for improvement of the machine efficiency and reduction of the kVA rating of the converter required for the machine supply. In the following, the machine operating principle is discussed and equivalent circuits suitable for the study of either steady-state or transient operation are derived. Finally, results of a computer simulation are used to discuss the machine behaviour when operated as direct drive motor in the electrical vehicle application.

2. MACHINE STRUCTURE

In the proposed axial-flux machine topology the stator winding is realised by means of series-connected coils which are placed side by side on a slotless core made from strip-iron wound in a toroidal fashion. The two PM rotor discs support Nd-Fe-B magnets which are used to drive flux across the machine airgaps. Since these intermediate rotor discs are merely used for the mechanical support of the magnets, light weight non-magnetic materials (e.g. aluminium) can be used for their construction thus enhancing the compactness and lightness of the machine. The two cage-rotor discs have a soft-iron toroidal core with radially-arranged slots to house copper bars. Copper rings are placed at both the inner and outer radius of the rotor toroidal core in order to connect all the bar ends among them and thereby accomplish a disc-shaped squirrel-cage winding. The machine structure is schematically shown in Fig. 2 in form of top view of a rectified cross-section. Paths of the airgap flux linkages are also shown in this figure.

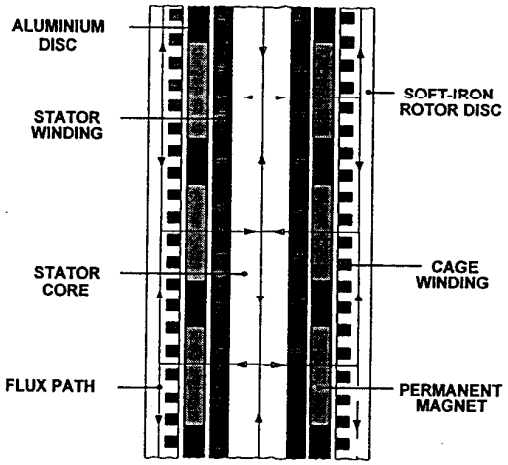

Fig. 2 Top view of the machine structure.

3. STUDY OF THE MACHINE OPERATION

By neglecting saturation and iron losses, the voltage and flux linkages equations may be derived starting from the equivalent circuit shown in Fig. 3 which relates to the magnetic quantities of the machine. In the following, machine quantities indicated with a boldface character are phasors, and the subscripts s, $r1$, $r2$ denote variables and parameters associated with the stator and the two cage rotors (e.g. named rotor 1 and rotor 2), respectively. An m subscript denotes variables and parameters

associated with the magnetizing paths, whereas variables and parameters associated with leakage paths are denoted by an *l* subscript. All the equations refer to machine parameters and variables expressed as per unit quantities.

3.1 Machine equivalent circuit

The magnetic circuit shown in Fig. 3 is drawn to retain the symmetry of the machine structure shown in Fig. 2. In this regard, it is useful to note that from the magnetic point of view the machine structure shown in Fig. 2 has only two airgaps, as both copper and permanent magnet materials have permeability very close to that of air. Thereby, the length of the magnetic airgaps of the machine is mainly determined by the thickness of the stator coils and of the permanent magnets since the two mechanical airgaps used for clearance is only a small part of the overall length of each magnetic airgap. Hence, in order to take into account the presence of permanent magnets in the machine airgaps, the circuit shown in Fig. 3 includes an MMF $\mathbf{F_{pm}}$ which represents the action exerted by each permanent magnet rotor disc to sustain the magnetizing flux in the related airgap (i.e., either ϕ_{m1} or ϕ_{m2}) in addition to the MMFs produced by the currents flowing in the stator and cage rotors windings (i.e. $\mathbf{F_s}$, $\mathbf{F_{r1}}$, $\mathbf{F_{r2}}$, respectively). For each machine airgap it is assumed that the flux produced by the permanent magnets links both stator and cage rotor. Hence, from Fig. 3 it can be written that:

$$\Phi_{m1} = \left(F_s + F_{pm} - F_{r1}\right) / \mathcal{R}_m \quad (1)$$

$$\Phi_{m2} = \left(F_s + F_{pm} - F_{r2}\right) / \mathcal{R}_m \quad (2)$$

and

$$\Phi_s = \Phi_{ls} + \Phi_{m1} + \Phi_{m2} \quad (3)$$

$$\Phi_{r1} = \Phi_{lr1} + \Phi_{m1} \quad (4)$$

$$\Phi_{r2} - \Phi_{lr2} + \Phi_{m2} \quad (5)$$

where

$$\Phi_{ls} = F_s / \mathcal{R}_{ls} \quad (6)$$

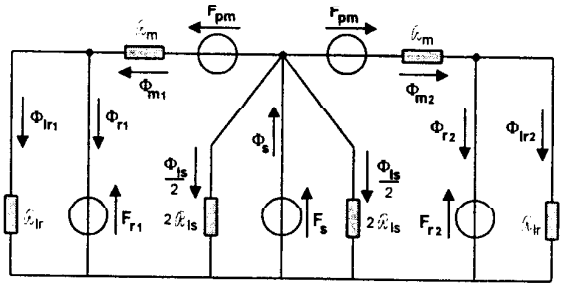

Fig. 3 Equivalent circuit related to magnetic quantities.

$$\Phi_{lr1} = F_{r1} / \mathcal{R}_{lr} \quad (7)$$

$$\Phi_{lr2} = F_{r2} / \mathcal{R}_{lr} \quad (8)$$

The flux linkages may be derived from the above equations and written in the form:

$$\Lambda_s = L_{ls} \cdot I_s + \Lambda_{m1} + \Lambda_{m2} \quad (9)$$

$$\Lambda_{r1} = L_{lr1} \cdot I_{r1} + \Lambda_{m1} \quad (10)$$

$$\Lambda_{r2} = L_{lr2} \cdot I_{r2} + \Lambda_{m2} \quad (11)$$

and

$$\Lambda_{m1} = L_m \cdot \left(I_s + I_{r1}\right) + \Lambda_{pm} \quad (12)$$

$$\Lambda_{m2} = L_m \cdot \left(I_s + I_{r2}\right) + \Lambda_{pm} \quad (13)$$

where Λ_{pm} is the flux linkage established at the airgap by the permanent magnets, L_m is the magnetizing inductance related to each magnetic airgap of the machine, L_{ls}, L_{lr1}, L_{lr2} are leakage inductances and I_s, I_{r1}, I_{r2} are the current flowing in the windings of the stator and cage rotors, respectively.

Since the instantaneous position of the permanent magnet rotors is used to determine the switching pattern of the inverter which supplies the machine stator winding, it is a convenient choice to write the machine voltage equations by considering a reference frame rotating with the permanent magnet rotors. The position of the reference frame is selected such that $\Lambda_{pm} = -j\lambda_{pm}$, i.e. the flux established by the permanent magnets only has a d-axis component. Thus, the voltage equations become:

$$V_s = R_s \cdot I_s + j\omega\Lambda_s + p\Lambda_s \quad (14)$$

$$0 = R_r \cdot I_{r1} + js_1\omega\Lambda_{r1} + p\Lambda_{r1} \quad (15)$$

$$0 = R_r \cdot \mathbf{I}_{r2} + js_2\Lambda_{r2} + p\Lambda_{r2} \qquad (16)$$

where p is the time-derivative operator, R_s, R_{r1}, R_{r2} are the machine windings resistances, ω is the machine supply frequency, s_1 and s_2 are the slips of the cage rotors and $\mathbf{V}_s$ is the supply voltage of the machine stator winding. The above voltage and linkage flux equations suggest the machine equivalent circuit shown in Fig. 4.

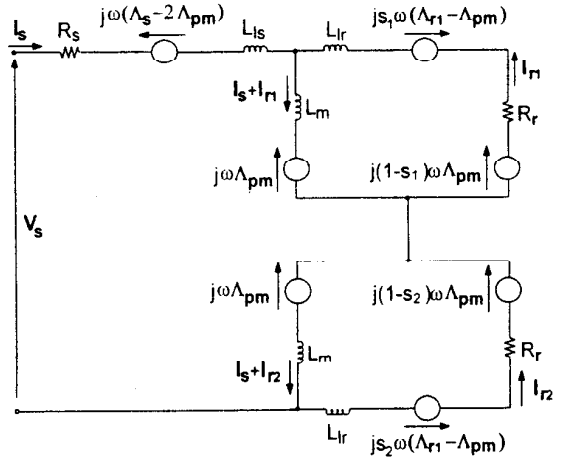

Fig. 4 Machine equivalent circuit with variables in a permanent magnet rotor reference-frame .

An expression for the electromagnetic torque acting on each cage rotor may be obtained by considering the expression of the per unit torque which is globally developed by the machine:

$$T_e = \omega_n \cdot \left(\lambda_{ds} i_{qs} - \lambda_{qs} i_{ds}\right) \qquad (17)$$

where ω_n is the machine rated frequency.

Under the assumption that the mechanical losses associated with the rotation of the permanent magnet rotors are negligible, eq. (17) gives an electromagnetic torque which is entirely transmitted from the stator to both the cage rotors (i.e., $T_e = T_{er1} + T_{er2}$), and thereby by using eq. (9) into (17) it is found:

$$T_{er1} = \omega_n \cdot \left(\lambda_{dm1} i_{qs} - \lambda_{qm1} i_{ds}\right) \qquad (18)$$

$$T_{er2} = \omega_n \cdot \left(\lambda_{dm2} i_{qs} - \lambda_{qm2} i_{ds}\right) \qquad (19)$$

By using (9)-(13), the above torque equations may be expressed in terms of variables associated with the machine cage rotors.They yield:

$$T_{er1} = \omega_n \cdot \left(\lambda_{qr1} i_{dr1} - \lambda_{dr1} i_{qr1} + \lambda_{qm1} \lambda_{pm} / L_m\right) \qquad (20)$$

$$T_{er2} = \omega_n \cdot \left(\lambda_{qr2} i_{dr2} - \lambda_{dr1} i_{qr2} + \lambda_{qm2} \lambda_{pm} / L_m\right) \qquad (21)$$

If the machine is used for the propulsion of the wheels of an electric vehicle and is operated along a straight path, the two cage rotors rotate at a same speed which is determined by the speed of the vehicle. In this case, the speed of the cage rotors is only related to the total electromagnetic torque by:

$$p\omega_r = \omega_n \left(T_e - T_l\right)/2H \qquad (22)$$

where T_l is the overall load torque at the axles of the wheels and H is the inertia constant of the vehicle. Hence, the slip value at which the cage rotors operate is found as:

$$s_1 = s_2 = s = \left(\omega - \omega_r\right)/\omega \qquad (23)$$

Whenever the vehicle enters a curved path the vehicle wheels are forced to rotate at different speeds with respect to the other, and this speed differential action exerted on the vehicle wheels results in a slip constraint for the machine cage rotors, as will be discussed. Eqs. (9)-(22) yield a machine model which is suitable for the study of the machine behaviour during either steady-state or transient running conditions.

3.2 Steady-state operation

The voltage equations which describe the machine steady-state operation are easily achieved in the phasor form by setting p = 0 into eqs. (14)-(16). The resulting voltage equations together with the flux linkage equations are represented by the machine equivalent circuit shown in Fig. 5.

As in conventional permanent magnet motor drives, for constant torque operation the machine is supplied by means of a rotor-position controlled CRPWM inverter which delivers at the stator input terminals a sinusoidal-waveform three-phase current with only a q-axis

component of desired amplitude. Thereby, in the following it is assumed that $\mathbf{I}_s = i_{qs}$ and $i_{ds} = 0$, and that steady-state operation of the machine is referred to running conditions with either $s_1=s_2$ or $s_1 \neq s_2$ depending on the vehicle mode of operation.

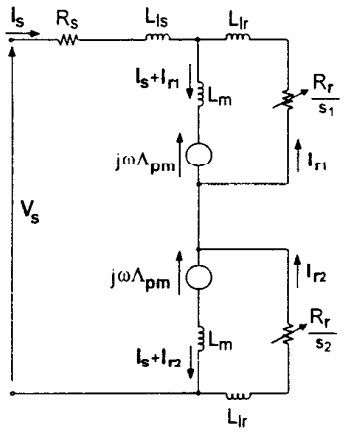

Fig. 5 Equivalent circuit for steady-state operation.

If $s_1=s_2$, then there is complete balance between the two airgaps of the machine and the two cage rotors share the same amount of the power delivered at the machine input terminals. In this case, the machine variables can be represented by the phasor diagram shown in Fig. 6A, where the subscripts 1 and 2 are omitted because of the loss of significance.

Steady-state running conditions with $s_1 \neq s_2$ occur whenever the vehicle propelled by the machine moves along a curved path, as schematically shown in Fig. 7. If s is an average slip related to the speed of the vehicle (i.e., s may be viewed as the slip of a dummy cage rotor which delivers the entire torque of the machine to drive a dummy wheel located at the center of the axle of the vehicle), the curve trajectory constrains the cage rotor driving the inner wheel to operate with slip $s+\Delta s$ whereas the cage rotor driving the outer wheel must rotate with slip $s-\Delta s$.

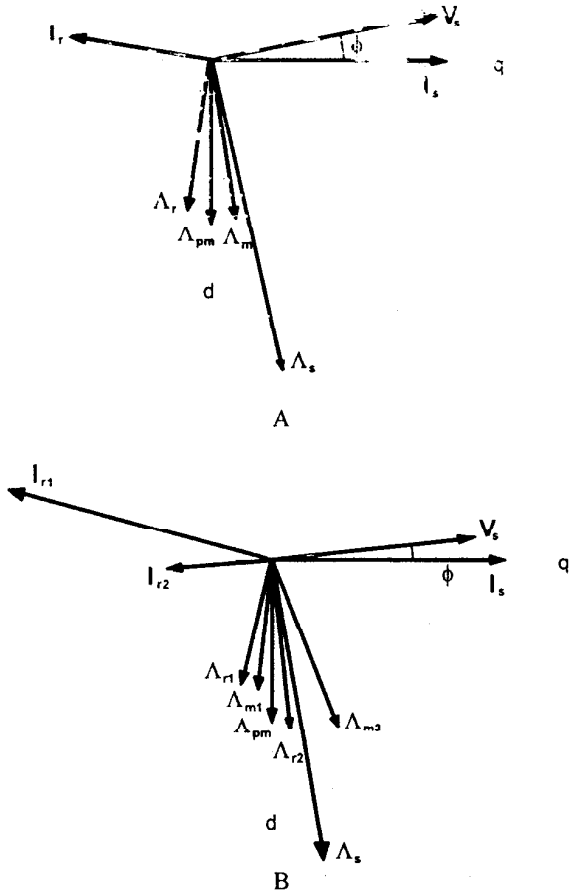

Fig. 6 Phasor diagrams related to machine steady-state operation: A. $s_1 = s_2$; B. $s_1 > s_2$

R : radius of the curve path; a : wheel axle length;
R_W: wheel radius; v : vehicle instantaneous speed;
ω : motor supply frequency; p : motor pairs of poles.

slip forced at the inner wheel:

$$s_i = 1 - \frac{p\, v_i}{\omega R_W} = 1 - \frac{p\, v}{\omega R_W}\left(1 - \frac{a}{R}\right) = s + \Delta s$$

slip forced at the outer wheel:

$$s_o = 1 - \frac{p\, v_o}{\omega R_W} = 1 - \frac{p\, v}{\omega R_W}\left(1 + \frac{a}{R}\right) = s - \Delta s$$

where:

$$s = 1 - \frac{p\, v}{\omega R_W} \quad \text{and} \quad \Delta s = \frac{a}{R}\,\frac{p\, v}{\omega R_W}$$

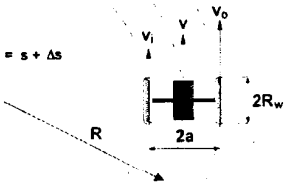

Fig. 7 Slip constraint in the machine cage rotors due to vehicle operation in a curved path.

As shown in Fig. 7, the differential slip Δs is mainly determined by the turning ratio a/R which for conventional vehicles having a = 0.6 can assume a value in the range from 0 (straight paths) to about 0.12 (a curved path with radius of about 5 m).

By considering a vehicle which moves at a given constant speed in a curved path, and assuming that the machine cage rotor labeled as 1 is driving the inner wheel of the vehicle, Fig. 6B shows the steady-state operation phasor diagram of machine significant quantities. In comparison with Fig. 6A, one can observe that the differential slip imposed by the curved path reflects on the current phasors of the cage rotors in terms of significant both difference of amplitude and phase shifting between them. This behaviour has a substantial effect on the magnetizing flux linkages at the two machine airgaps.

As the phasor $\mathbf{I}_{r1}$ moves clockwise and its amplitude increases, the current $\mathbf{I}_s+\mathbf{I}_{r1}$ mostly becomes a negative d-axis current and substantially acts to offset the flux linkage established at the airgap by the permanent magnets. On the other hand, $\mathbf{I}_{r2}$ is forced to both move counter-clockwise and reduce in amplitude, so that the current $\mathbf{I}_s+\mathbf{I}_{r2}$ mostly becomes a q-axis current. As a result, the phasor of the magnetizing flux linkage at the airgap 2 moves counter-clockwise with a relatively small increment of its d-axis component.

Of course, the above considerations have an impact on the electromagnetic torques transmitted to the two cage rotors of the machine. By setting $i_{ds} = 0$ and considering i_{qs} as a constant in equations (18)-(19), it is found that whenever the vehicle enters a curved path the torque transmitted to the inner wheel cage rotor decreases, whereas the torque transmitted to the cage rotor driving the outer wheel practically remains constant. Hence, this results in a decrease of the global torque developed by the machine. and thereby for operation in a curved path with constant speed of the vehicle a slight decrease of the active power required at the machine input terminals occurs. On the other hand, because of a reduction of the overall magnetization of the machine airgaps the voltage required at the machine input decreases and there is a slight increase of the power factor at the input terminals, as it can be noted from a comparison of the phasor diagrams A and B shown in the preceding Fig. 6.

3.3 Computer simulation

In order to achieve a deeper insight into the machine performance when operated as an "electromagnetic differential gearbox", the machine model developed above was used for a computer simulation of the machine operation with a vehicle running in a curved path. To this end, an ACSL numerical procedure was developed on a PC by considering the first-tentative machine data and parameters given in Appendix.

With reference to operation with a vehicle running on a curved path characterized by a turning ratio of about 0.05, Figs. 8, 9, 10 and 11 show computer traces which refer to significant machine quantities such as speed of each rotor, amplitude of the cage rotors currents and of the airgap magnetizing flux linkages, electromagnetic torques transmitted to the cage rotors, respectively. The numerical procedure simulates a vehicle running on a straight path with the machine being operated at s=0.045 with commanded input current i_{qs} = 1 p.u.. After about 1 s of the simulation time interval the vehicle enters a curved path, and this is covered within a 4 s time duration with no changes in the commanded input current. Turning of the vehicle wheels to either enter or escape the curved path takes about 1.5 s, and during this time interval the differential slip between the vehicle wheels is linearly increased from 0 up to the value imposed by the radius of the path.

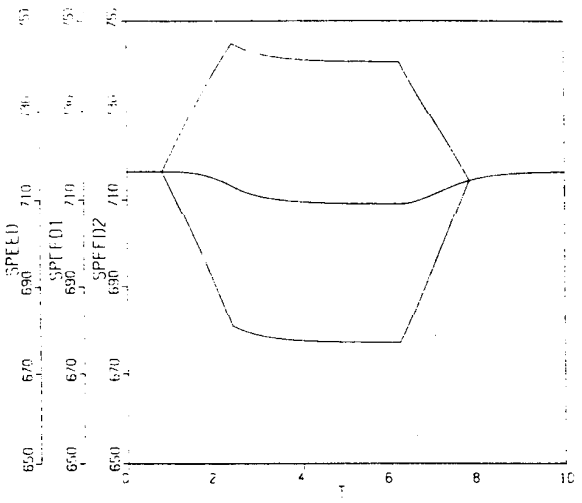

Fig. 8 Speed transient for operation along a curved path: SPEED: average speed; SPEED1, SPEED2: speeds of the cage rotors

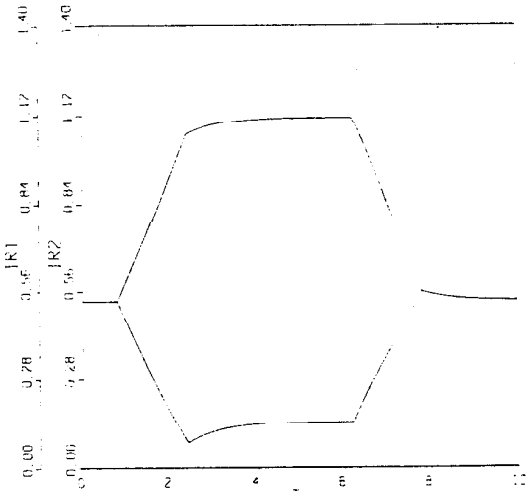

Fig. 9 Transient of the currents in the cage rotors corresponding to Fig. 8

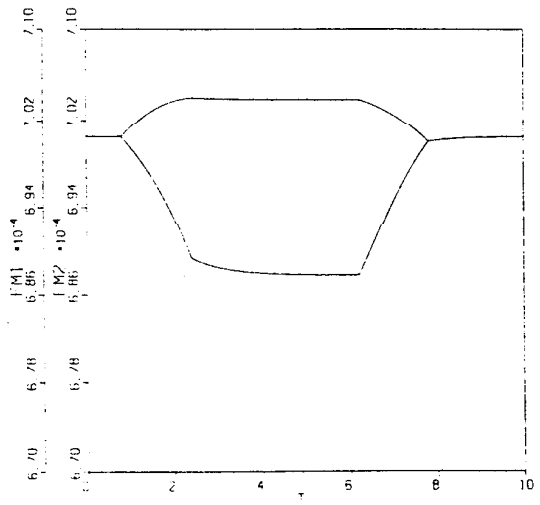

Fig. 10 Transient of the magnetizing flux linkages corresponding to Fig. 8

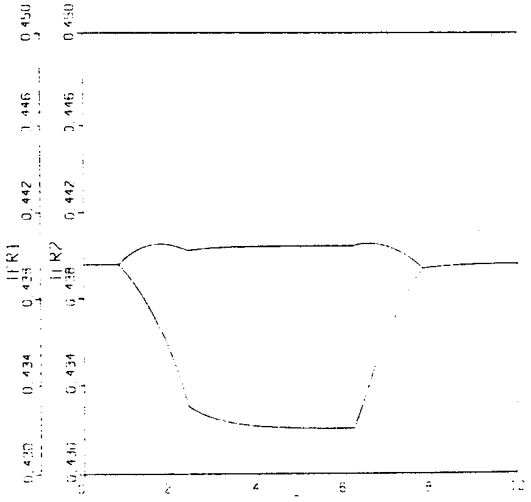

Fig. 11 Transient of the electromagnetic torques corresponding to Fig. 8

The computer results clearly demonstrate the capability of the machine in operating as a differential gearbox while driving the vehicle wheels along a curved path. As mentioned previously, this machine behaviour is mainly due to the armature reaction of the inner wheel cage rotor, which partially offsets the flux linkage established at the airgap by the permanent magnet flux and thereby reduces the transmitted electromagnetic torque. While the achievement of the desired differential behaviour of the machine takes advantage from the inner wheel rotor armature reaction, this is normally not of concern for a possible demagnetization of the permanent

magnet rotor discs, since the machine has quite large airgaps and thereby the related magnetizing inductances are of the same order of the leakage inductances associated with the cage rotors themself.

4. CONCLUSIONS

The electric vehicle of the future are expected to be propelled by direct drive wheel motors for a more efficient powertrain. Concerning the electric vehicle application, this paper has presented preliminary results of a study of an original permanent magnet axial-flux machine topology which allows one to combine in a single motor drive the function of both the engine and the differential required in conventional vehicles.

One significant advantage of the proposed motor drive with respect to twin-motor wheel direct drive arrangements is that only a single power converter is required for the machine supply. In addition, because of the permanent magnet excitation of the machine airgaps, the proposed motor drive operates at nearly unity power factor and this reflects in a reduction of the kVA rating needed for the converter used for the machine supply. Design of a prototype of the proposed machine structure is being under development and experimental results taken from this prototype machine will be reported in a future paper.

REFERENCES

[1] F. Caricchi, F. Crescimbini, A. Di Napoli, O. Honorati, T.A. Lipo, G. Noia, E. Santini, "Development of an IGBT Inverter Driven Axial-Flux PM Synchronous Motor Drive", Proceedings of the 4th EPE Conference, 1991, Vol. 3, pp. 482 - 487.

[2] F. Caricchi, F. Crescimbini, L. Fedeli, G. Noia, "Design and Construction of a Wheel-Directly-Coupled Axial-Flux PM Motor Prototype for EVs", Proceedings of the 1994 IEEE-IAS Annual Meeting. Denver (USA), 2-7 October 1994.

[3] T.A. Lipo, "Analog Computer Simulation of an Axially Aligned Two Rotor AC Machine", M.S.E.E. Thesis, Marquette University, Wisconsin (USA), 1964.

[4] D. Platt, B.H. Smith, "Twin Rotor Drive for an Electric Vehicle", IEE Proceedings, Part B, Vol. 140, No. 2, March 1993, pp. 131-138.

[5] F. Caricchi, F. Crescimbini, E. Santini, "Axial-Flux Electromagnetic Differential Induction Motor", Proceedings of the 7th IEE Seventh International Conference on Electrical Machines and Drives, Durham (UK), 10 13 September 1995, pp. 1-5.

Appendix

Machine data and per unit parameters used for computer simulation:

Rated frequency	100 Hz
Rated power	20 kW
Rated voltage (line-to-line)	380 V
Pairs of poles	8
Stator winding resistance (R_s)	9.00×10^{-2} pu
Rotor winding resistance (R_r)	3.75×10^{-2} pu
Stator leakage inductance (L_{ls})	0.55×10^{-4} s
Rotor leakage inductance (L_{lr})	0.83×10^{-4} s
Magnetizing inductance (L_m)	0.76×10^{-4} s
Permanent magnet flux (λ_{pm})	7.00×10^{-4} s